Science of the Total Environment 886 (2023) 163767

Contents lists available at ScienceDirect

Science of the Total Environment

journal homepage: www.elsevier.com/locate/scitotenv

# Predicting human neurotoxicity of propylene glycol methyl ether (PGME) by implementing *in vitro* neurotoxicity results into toxicokinetic modelling

E. Reale [a], J. Sandstrom [b,e], M. Culot [c], J. Hechon [d], S. Wellens [c], M. Heymans [c], F. Tschudi-Monnet [e], D. Vernez [a], N.B. Hopf [a,*]

[a] Center for Primary Care and Public Health (Unisanté), Route de la Corniche 2, 1066 Epalinges-Lausanne, Switzerland
[b] Swiss 3R Competence Centre, Hochschulstrasse 6, CH-3012 Bern, Switzerland
[c] Univ. Artois, UR 2465, Laboratoire de la Barrière Hémato-Encéphalique (LBHE), F-62300 Lens, France
[d] Institut Universitaire de Santé au Travail (IST), Rue du Bugnon 19, 1005 Lausanne, Switzerland
[e] Swiss Centre for Applied Human Toxicology (SCAHT), University of Basel, Missionsstrasse 64, CH-4055 Basel, Switzerland

## HIGHLIGHTS

- *In vivo* neurotoxicity is seldom assessed before placing solvents on the market.
- Neurotoxicity can be assessed by integrating *in vitro* and *in silico* methods.
- Glycol ethers (GE) pass easily through the blood-brain barrier.
- GE had few adverse effects on brain cells but activated the CNS immune response.
- TK models are suitable to extrapolate from NOAEC to corresponding air concentrations.

## GRAPHICAL ABSTRACT

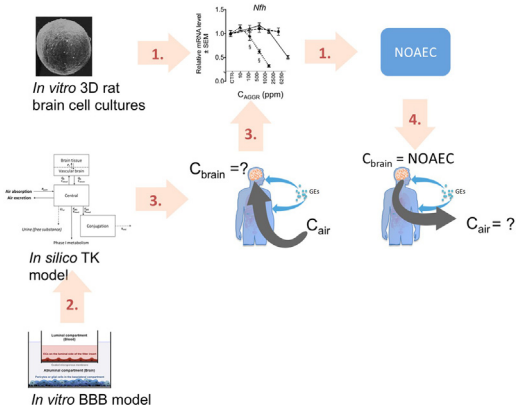


## ARTICLE INFO

Editor: Henner Hollert

*Keywords:*
Glycol ethers
CNS
PBPK
IVIVE
1-Methoxypropan-2-ol
Solvent neurotoxicity

## ABSTRACT

Although organic solvents have been associated with CNS toxicity, neurotoxicity testing is rarely a regulatory requirement. We propose a strategy to assess the potential neurotoxicity of organic solvents and predict solvent air concentrations that will not likely produce neurotoxicity in exposed individuals. The strategy integrated an *in vitro* neurotoxicity, an *in vitro* blood-brain barrier (BBB), and an *in silico* toxicokinetic (TK) model. We illustrated the concept with propylene glycol methyl ether (PGME), widely used in industrial and consumer products. The positive control was ethylene glycol methyl ether (EGME) and negative control propylene glycol butyl ether (PGBE), a supposedly non-neurotoxic glycol ether. PGME, PGBE, and EGME had high passive permeation across the BBB (permeability coefficients ($P_e$) $11.0 \times 10^{-3}$, $9.0 \times 10^{-3}$, and $6.0 \times 10^{-3}$ cm/min, respectively). PGBE was the most potent in *in vitro* repeated neurotoxicity assays. EGME's main metabolite, methoxyacetic acid (MAA) may be responsible for the neurotoxic effects reported in humans. No-observed adverse effect concentrations (NOAECs) for the neuronal biomarker were for PGME, PGBE, and EGME 10.2, 0.07, and 79.2 mM, respectively. All tested substances elicited a concentration-dependent increase in pro-inflammatory cytokine expressions. The TK model was used for *in vitro-to-in vivo* extrapolation from PGME NOAEC to corresponding air concentrations (684 ppm). In conclusion, we were able to predict air concentrations that would not likely result in neurotoxicity using our strategy. We confirmed that the Swiss PGME occupational exposure limit (100 ppm) will not likely produce immediate adverse effects on brain

* Corresponding author.
*E-mail address:* Nancy.Hopf@unisante.ch (N.B. Hopf).

http://dx.doi.org/10.1016/j.scitotenv.2023.163767
Received 13 February 2023; Received in revised form 17 April 2023; Accepted 23 April 2023
Available online 6 May 2023

cells. However, we cannot exclude possible long-term neurodegenerative effects because inflammation was observed *in vitro*. Our simple TK model can be parameterized for other glycol ethers and used in parallel with *in vitro* data for systematically screening for neurotoxicity. If further developed, this approach could be adapted to predict brain neurotoxicity from exposure to organic solvents.

## 1. Introduction

Glycol ethers (GE) are amphiphilic liquids, widely used as organic solvents in oil-water formulations such as paints, inks, and cleaning products. The human body readily absorbs GEs by inhalation, dermal absorption and ingestion. Typical exposures are associated with skin absorption and inhalation during painting and cleaning. GEs are classified into two main chemical families: ethylene glycol-derived ethers (EGEs) and the propylene glycol-derived ethers (PGEs). EGEs were widely used from 1930 to1980, but in recent decades their production has dropped drastically because of their toxicity to the developing foetus, testicular tissue, thymus, blood, and blood forming tissues (Crag, 2012). These toxic effects are due to EGEs' main metabolite, the alkoxyacetic acid, and are not observed for PGEs. PGEs' main effect is an increase in liver and kidney weight (ECETOC, 2005a). Hence, PGEs are considered a safer alternative to EGEs and have gradually replaced them in commercial products.

PGEs have two isomers, containing either a secondary (α-isomer) or a primary (β-isomer) alcohol. The β-isomers are impurities (<0.5 %) of the commercial compounds (α-isomers). PGE β-isomers main metabolic pathway is similar to EGEs: the oxidation of their primary alcohol group into the metabolite alkoxypropionic acid, *via* alcohol and aldehyde dehydrogenases (ECETOC, 2005a) (Fig. 1). The PGE α-isomers cannot be metabolized into a carboxylic acid, since the hydroxyl group is a secondary alcohol. PGEs' α-isomer is mainly metabolized by microsomal CYP mixed function oxidase (MFO) into propylene glycol, which enters intermediary metabolism *via* the tricarboxylic acid (TCA) cycle, leading to exhaled carbon dioxide ($CO_2$). A secondary metabolic pathway is the conjugation with sulphate and glucuronid acid. These metabolites are excreted in urine. Occupational exposure limits (OEL) exist for a few GEs and are mainly based on skin irritation endpoint for PGEs, and reprotoxicity for EGEs.

In acute scenarios, GE exposure can cause unspecific central nervous system (CNS) depression (Cosmetic Ingredient Review Expert Panel, 2008), which is typical of organic solvents (Dick, 2006; Evans and Balster, 1991; Ridgway et al., 2003; Sainio, 2015). More specifically, ethylene glycol methyl ether (EGME) has been recognized for CNS effects in humans (ECETOC, 2005a) at much higher exposures than the current OEL (1 ppm). For two EGs main substitutes on the market, propylene glycol methyl ether (PGME) and propylene glycol n-butyl ether (PGBE), CNS depression occurs at higher concentrations than those observed for irritation (Miller et al., 1984; Reijnders and Verschuuren, 1987; Spencer et al., 2002; Stewart et al., 1970). In general, subacute studies in animals did not indicate any neurological effects. As a consequence, the interest in GEs neurotoxicity has dropped. However, neurological effects have not been systematically examined for glycol ethers. Out of >80 registered GEs, only TEGME (CAS:112-35-6) has undergone an OECD TG (TG408) test, and only motor activity and histopathology were included as endpoints. For few GEs where neurotoxicity was reported in the registration dossier, data were very limited. Therefore, considering that GEs are widely used organic solvents, and that for many GEs there is no toxicological information, GEs' possible neurotoxicity cannot be ruled out and needs to be explored. Furthermore, neurotoxic effects of chronic exposure could be of further concern as the link between chronic exposure to organic solvent mixtures, including GEs, and encephalopathy has been well-documented (Keski-Säntti et al., 2010; Mikkelsen et al., 1988; Triebig et al., 1992).

Different types of *in vitro* organ-specific toxicity tests exist and may provide an alternative to traditional animal experiments. In the AcuteTox EU project, the aggregating rat brain cell cultures (AGGR) underwent a pre-

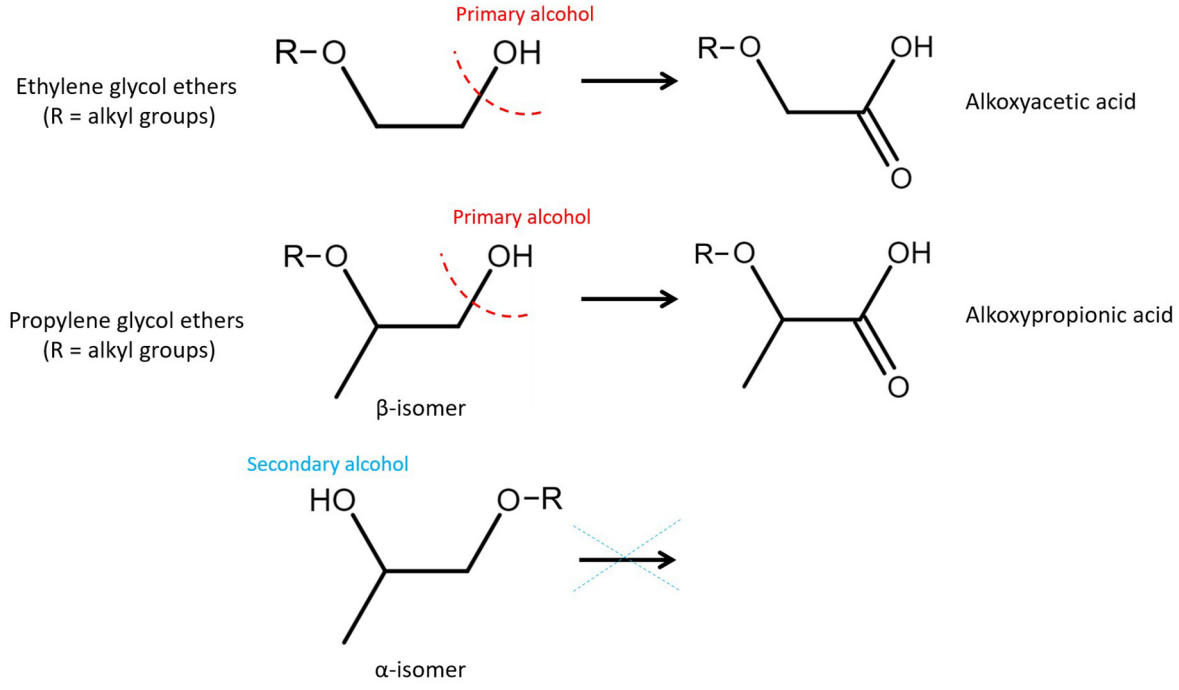


**Fig. 1.** Generic molecular structures of ethylene glycol ethers and propylene glycol ethers. Primary alcohol groups are metabolized to the corresponding acid, which has been reported to be reprotoxic.

validation test for its capacity to recognize acute neurotoxicity using a training set of 57 chemicals and 32 blind-coded chemicals for valuation (Kinsner-Ovaskainen et al., 2013; Prieto et al., 2013; Zurich et al., 2013). The AGGR proved to offer a sensitive *in vitro* assay for predictive assessment of acute human brain-specific neurotoxic effects by using a combination of the IC20 of the 3T3/NRU cytotoxicity test system and summary values obtained through gene expression analysis of the four genes heat-shock protein 32 (HSP-32), neurofilament heavy chain (NF-H), glial fibrillary acidic protein (GFAP) and myelin basic protein (MBP).

*In vitro* data are not directly interpretable for human exposures, and need to be put in context with human physiology and kinetics (adsorption, distribution, metabolism, excretion). By combining *in vitro* data with *in silico* kinetic modeling, we can estimate exposures corresponding to *in vivo* target-organ concentrations that produced neurotoxicity *in vitro*. This combined approach is one way of carrying out an *in vitro*-to-*in vivo* extrapolation (IVIVE) (Chang et al., 2022). IVIVE has been used to predict the exposure levels for neurotoxicity of eight known neurotoxicants (Blaauboer, 2001; DeJongh et al., 1999), for embryotoxicity of four EGEs and their alkoxyacetic acid metabolites (Louisse et al., 2010; Verwei et al., 2006). More recently, Kasteel et al. (2021) used IVIVE to predict neurologically active doses of baclofen, an antispastic drug. Over the past decade there has been a burst of publications on IVIVE (Loizou et al., 2021; Noorlander et al., 2022; Punt et al., 2019; Shi et al., 2020; Wang et al., 2017), and IVIVE is beginning to gain acceptance in the risk assessment of chemicals domain (Chang et al., 2022).

Our aim was to predict an exposure concentration for PGME that would not induce neurotoxicity in humans by integrating repeated-dose *in vitro* data with *in silico* data. Our first objective was to obtain concentration-response curves using AGGR to determine if PGME could potentially produce adverse effects in the brain, and at what concentrations. *In vitro* neurotoxicity testing was also done on EGME, as a positive control, and on PGBE, a widely used and supposedly non-neurotoxic GE (ECETOC, 2005b), for comparison. Our second objective was to predict brain concentrations upon exposure to PGME vapors using an *in silico* toxicokinetic (TK) model. Finally, by combining our *in vitro* data and *in silico* predictions, our last objective was to calculate an air concentration for PGME corresponding to the *in vitro* no-observed adverse effect concentrations (NOAEC) for neurotoxicity. The overall goal was to calculate occupational exposure levels for neurotoxicity incorporating 8 h daily exposures (cumulative) from inhalation to vapors.

## 2. Material and methods

### 2.1. Chemicals and reagents

Standard analytical PGME (CAS# 107-98-2), PGBE (CAS# 5131-66-8), EGME (CAS# 109-86-4), and propylene glycol propyl ether (PGPE) (CAS# 1569-01-3) used as internal standard (IS), were obtained from Sigma-Aldrich (Buchs, Switzerland). Sodium sulphate was purchased from Merck (Darmstadt, Deutschland). Water was purified *in situ* (Millipore system, Merck, Darmstadt, Germany). Hank' balanced salt solution (HBSS from Sigma – Ref H8264) contained 10 mM HEPES (HEPES Solution from Sigma – Ref H0887). Polycarbonate filter inserts with 0.4 μm filter pore size and a surface of 1.1 $cm^2$ (*i.e.* 12-well inserts) were from Corning Incorporated (NY, NY, USA). The upper side was coated with 1/48e diluted Matrigel (BD Biosciences, Le Pont-deClaix, France). Sodium fluorescein (NaFlu) was obtained from Sigma Aldrich (Darmstadt, Germany). Ringer-HEPES (RH) solution was composed of 150 mM NaCl, 5.2 mM KCl, 2.2 mM $CaCl_2$, 0.2 mM $MgCl_2{\cdot}6H_2O$, 6 mM $NaHCO_3$, 5 mM HEPES, 2.8 mM glucose (pH 7.4); all reagents were obtained from Sigma-Aldrich (Saint Quentin Fallavier, France).

### 2.2. AGGR and in vitro neurotoxicity testing

Aggregating brain cell cultures were prepared from the whole brain of 16-day embryonic rats (Sprague Dawley, Janvier, France) as previously described in detail (Honegger et al., 2011). The day of primary culture preparation equals day-*in-vitro* (DIV) 0. The brain cell aggregates were subcultured in a chemically defined medium under constant gyratory agitation (80 rotations per minute, rpm) at 37 °C in an atmosphere of 10 % $CO_2$ and 90 % humidified air. Media was freshly replenished every 3rd day until DIV 14, and every second day thereafter. Replicate cultures were prepared by randomizing and aliquoting the free-floating aggregates of the original cultures. Three technical replicates were prepared per test concentration and experiments were repeated at least three times on three independent primary culture preparations. Treatment was started at DIV31, when cultures reached a highly matured state comprising all major brain cells: neurons, astrocytes, oligodendrocytes, as well as microglia. Over a five-day period, simulating the duration of a working week, the neural microtissues were exposed to a daily supplementation of 25 μL stock solution of glycol ether, which was directly added to the 5 mL total volume of culture medium. All the materials used in the tests with AGGR were made of glass to reduce potential adsorption of glycol ethers (Borgatta et al., 2021).

In a preliminary phase, we tested pure substances separately, EGME and PGBE, at two different concentrations: 500 and 6250 ppm. These concentrations corresponded to the minimum and half of the maximum volume of tested substance that can be added to the cell cultures for practical reasons, 2 μL and 25 μL respectively. In a second phase, we lowered the concentrations by diluting the glycol ethers in water, in order to avoid cytotoxic levels. Hence, the three glycol ethers were prepared in 100-fold stock solutions by serial dilutions and final nominal culture media concentrations at the beginning of the treatment ranged from 0 (vehicle control) to 1000 ppm. A higher concentration of 6250 ppm PGME was obtained by adding 25 μL of pure PGME to the cell cultures. The dilution factors in water (*v*/v) and the final concentrations of the three glycol ethers in the cell cultures are illustrated in Table 1. Aggregates were harvested by washing twice in cold phosphate buffered saline and pellet was subsequently frozen on dry ice and stored at −80 °C until further processing.

#### 2.2.1. Semi-quantitative real-time PCR

RNA was extracted using the RNeasy kit (Qiagen), following manufacturer's guidance. Reverse transcription was performed with the High Capacity cDNA Reverse Transcription Kit (Applied Biosystems) using 2 μg of total RNA per reaction. The expression of *Act(Sybr)* (fw 5′-ccctggctcctagcaccat-3′, rev 5′- tagagccaccaatccacacaga-3′), *Nefh* (fw 5′-caggacctgctcaacgtcaa-3′, rev 5′-cttcgccttccaggagttttct-3′), *Gfap* (fw 5′-ccttagcctgcgaccttgag-3′, rev 5′-gcgcatttgcctctccaa-3′), *Mbp* (fw 5′-gcacgctttccaaaatctttaag-3′, rev 5′-agggaggctctcagcgtctt-3′) and *Hsp32* (fw 5′- aggtgtccagggaaggcttt-3′, rev 5′-tccagggccgtatagatatggt-3′) was quantified using Power SYBR Green (Applied Biosystems), with a total of 3.2 ng of cDNA per real-time PCR reaction. Expressions of *Il-1β* (Rn00580432_m1), *Il-6* (Rn99999011_m1), *Tnf-α* (Rn99999017_m1), and *Infγ* (Rn00594078_m1) were quantified with the

**Table 1**
Nominal concentrations in parts per million (ppm) of the three glycol ethers tested for effect on *in vitro* brain cells in the 3D whole rat brain cell cultures. In most cases, glycol ethers were diluted in water so that the same volume of 25 μL was added to all cultures.

| Substance | Water dilution (*v*/v) | Volume added to cell cultures (μL) | Nominal concentration in cell cultures (ppm or μL/L) | Nominal concentration in cell cultures (mM) |
|---|---|---|---|---|
| Control | | 0 | – | – |
| EGME | 8.7 % | 25 | 500 | 6.34 |
| | 66.7 % | 25 | 2500 | 31.70 |
| PGBE | 0.2 % | 25 | 10 | 0.07 |
| | 1.6 % | 25 | 100 | 0.67 |
| | 8.7 % | 25 | 500 | 3.33 |
| | 19.0 % | 25 | 1000 | 6.66 |
| PGME | 1.6 % | 25 | 100 | 1.02 |
| | 8.7 % | 25 | 500 | 5.10 |
| | 19.0 % | 25 | 1000 | 10.20 |
| | (pure) | 25 | 6250 | 63.73 |

Taqman gene expression assay (Applied Biosystems), following the manufacturers protocol and using a total quantity of 50 ng cDNA per reaction. Internal control gene β-actin (*Actb*) was used both for SYBR Green and Taqman detection at a total of 3.2 ng cDNA per reaction. For each primer pair reaction efficacy was tested and allowed the use of the ΔCt method for calculations (Livak and Schmittgen, 2001).

#### 2.2.2. Statistical analysis

Normality of data sets distribution was determined with the D'Agostino-Pearson omnibus normality test. Subsequently, multiple *t*-tests, followed by Sidak-Bonferroni correction for multiple comparisons were applied to determine statistically significant differences in gene expression upon equal concentration treatment with the different glycol ethers.

### 2.3. In vitro determination of CNS distribution parameters

#### 2.3.1. Ethics

The permit allowing experimentation on animals at the University of Artois (UART) is n° B62–498-5. All animal experiments were conducted following the EU Directive 2010/63/EU about animal protection and welfare.

#### 2.3.2. Plasma protein and brain tissue binding

Rat brain homogenate solution was prepared from brains of drug-naïve Sprague-Dawley rats (obtained from Janvier, Le Genest-St. Isle, France) homogenized using a glass Dounce homogenizer in 2 volumes of HBSS containing 10 mM HEPES at pH 7.4 and frozen at −20 °C until further use. Human plasma was acquired from the Etablissement Français du Sang (EFS).

The Rapid Equilibrium Dialysis (RED) Device (Thermofisher, Rockford, IL, USA) was used with an 8-kDa cut-off cellulose membrane to determine the unbound fraction in plasma ($f_{u,p}$) and brain ($f_{u,b}$). $f_{u,b}$ determined in rat brain tissue can be used as a surrogate for binding in other species (Di et al., 2011; Ryu et al., 2020). The test compounds were diluted at 10 and 20 μg/mL in either human plasma or rat brain homogenate solution and 300 μL of each solution was distributed in the donor chamber of the RED Device and dialyzed ($n = 3$) for 5 and 7 h on an orbital shaker (Polymix, Kinematica, city, country) at 250 RPM at 37 °C against 500 μL of HBSS (in the receiver chamber). Following incubation, aliquots were removed from the respective donor and receiver chambers from triplicate equilibrium dialysis chambers and transferred to a 96-well sampling plate, which had been frozen (−20 °C) till analysis by mass-spectrometry (see chapter 2.3.4 Quantification of glycol ethers). $f_{u,b}$ and $f_{u,p}$ were calculated based on compound concentration in donor and receiver chamber at equilibrium. $f_{u,p}$ was calculated from the ratio of the compound concentration in the buffer to the concentration of the compound in the plasma. $f_{u,b}$ was calculated according to the following formula introduced by Kalvass et al. (2007):

$$f_{u,b} = \frac{1}{1 + D\left(\frac{1}{f_{u,hD}} - 1\right)}$$

where D is the dilution of the brain homogenate (i.e. 3 times in HBSS) and $f_{u,hD}$ is the fraction of unbound compound in rat brain homogenate obtained according to the formula:

$$f_{u,hD} = \frac{C_{homogenate}}{C_{buffer}}$$

with $C_{homogenate}$ and $C_{buffer}$ the respective concentration of compound in homogenate and buffer.

#### 2.3.3. BBB permeability in a human in vitro model

The human *in vitro* BBB model derived from hematopoietic stem cells was prepared as previously described (Cecchelli et al., 2014a). Tissue culture inserts (12-well format, 1.12 $cm^2$, polycarbonate membrane, 0.4 μm pore size, Corning, New York, USA) were coated with Matrigel. The permeations across those inserts with and without brain-like endothelial cells were determined for each test compound.

Compounds were dissolved at 20 μg/mL in Ringer-Hepes (RH) containing sodium fluorescein (NaFlu) at 1 μM and 500 μL were added to the luminal (donor) compartment of the BBB model. The abluminal (receiver) compartment was filled with 1.5 mL of RH. After 60 min at 37 °C, an aliquot from each donor and receiver compartment was withdrawn and stored below −65 °C until analysis. All experiments were performed at least in triplicate.

Endothelial permeability coefficients ($P_e$, cm/min) for each test compound and for NaFlu were calculated as follows. For each replicate (control inserts without cells and inserts with cells), the clearance was calculated according to the following equation:

$$\text{Clearance } (\mu L) = C_R V_R / C_D$$

where $C_R$ and $V_R$ are the concentration and volume in the receiver compartment, respectively, and $C_D$ is the initial concentration in the donor compartment. The mean cleared volume was plotted as a function of time, and the slope was estimated by linear regression analysis. Permeability-surface area products (PS, $cm^3$/min) and $P_e$ values were subsequently calculated according to the following equations:

$$\frac{1}{PS_{total}} - \frac{1}{PS_{filter}} = \frac{1}{PS_e}$$

$$\frac{PS_e}{A} = P_e$$

where $PS_{total}$ was the slope of the clearance curve of cell monolayers with filter inserts, $PS_{filter}$ was the slope of the clearance curve of control filter inserts without cells, $PS_e$ was the slope of the clearance curve of the endothelial monolayers, and A was the surface area of the filter membrane.

Compound loss caused for example by adsorption on transwell plates, metabolism in the cells or insolubility of the compound was assessed by calculating the recovery (mass balance) according to the equation:

$$\text{Recovery } (\%) = (C_{Df} V_D + C_{Rf} V_R)/(C_{D0} V_D) \text{ x } 100$$

where $C_{Df}$ was the final concentration of the compound in the donor; $C_{Rf}$ was the final concentration of the compound in the receiver compartment; $C_{D0}$ was the initial concentration in the donor compartment; $V_D$,$V_R$ were the volumes in the donor and receiver compartments, respectively.

#### 2.3.4. Quantification of glycol ethers

Stock standard solutions were prepared by dissolving 20 mg of each glycol ether PGME, EGME and PGBE in 10 mL of water to obtain final concentrations of 2 mg/L. Stock standard solution of internal standard (IS) was prepared by diluting 20 mg of PGPE in 10 mL of water. The stock solutions were stable for 1 month when stored at 5–8 °C. IS and standard work solutions were prepared by diluting 200 μL of stock standard solution in 10 mL of water and stored at 5–8 °C for a week. A calibration was prepared in two steps to use the minimum amount of matrices used in the *in vitro* BBB model, and applying the same dilution factor for all calibration standards. Eight calibration standards were prepared in the range 0.1–50 mg/L in water, then diluted 10-fold in the biological matrix to obtain 8 calibration points in the range 0.01–5 mg/L (range of the study). Analysis was performed using a Thermo Scientific™ GC–MS/MS instrument (Thermo, Brechbuehler AG, Schlieren, Switzerland). A TRACE™ 1300 gas chromatographer (GC) was equipped with a TriPlus RSH™ autosampler and coupled with a TSQ 8000 triple quadrupole mass spectrometer (MS/MS) operating at 70 eV. The temperatures of the transfer line and of the ion source were 300 and 230 °C, respectively. Samples underwent a solid-phase microextraction (SPME) on a Carboxen / Polydimethylsiloxane fibre (CAR/PDMS fibre, $d_f$ 85 μm, needle size 24 ga, Supelco, Sigma Aldrich, Buchs, Switzerland). The compounds were separated with a capillary column (Zebron ZB-FFAP FFAP, 20 m × 0.18 id, 0.36 μm, Brechbuehler AG, Schlieren, Switzerland) with helium as the carrier gas. Range of linearity ($R^2 \geq 0.99$) was 0.01–2 mg/L in urine, blood and rat brain homogenate

for PGME; 0.01–5 mg/L in urine, 0.01–2 mg/L in blood, and 0.05–2 mg/L in rat brain homogenate for EGME; 0.01–5 in urine, and 0.01–2 in blood and rat brain homogenate for PGBE. The lower limit of quantification (LLOQ) was the lowest point of the calibration curve. At the LLOQ, precision (CV %) and accuracy (% deviation from nominal concentration) were calculated for three replicates and both were < 20 %.

### 2.4. PGME toxicokinetic model

#### 2.4.1. Model development and calibration

We used as a starting point the compartmental TK model for PGME used by Hopf et al. (2012). Briefly, their model assumed that PGME absorption occurs only by inhalation, and consisted of a central compartment for the distribution of PGME in the body. PGME underwent phase I and phase II metabolism (respectively, *o*-demethylation into propylene glycol, and conjugation with glucuronide and sulphate). Metabolism was assumed to follow Mikaelis-Menten kinetics. In urine, PGME can be quantified in its free and conjugated (*e.g.* glucuronidated) forms. Therefore, urinary excretion was modelled for free PGME as well as for total (sum of free and conjugated forms) PGME. Hopf et al. (2012) and Tomicic and Vernez (2014) showed that urinary PGME concentrations simulated with this simple model were in good agreement with experimental data of volunteers exposed to PGME vapors in an exposure chamber for 6 h.

We further developed this model to predict brain concentrations upon a simulated exposure to vapors of PGME. Concentration in blood was determined by dividing the central compartment concentration by the central compartment/blood partition coefficient ($P_{cb}$). Brain was modelled as a membrane-limited compartment (Fig. 2) to account for the presence of the BBB (Geldof et al., 2008). The brain compartment was composed of two sub-compartments, one for the brain vascular space (VB) and one for extravascular or tissue part of the brain (EVB). PGME uptake in EVB sub-compartment was assumed to follow passive diffusion with no carrier-mediated effects. Passive diffusion into the EVB was regulated by BBB permeability ($P_e$) determined by our *in vitro* BBB model. Chemicals in blood exist in two forms, bound to plasma proteins and unbound; similarly, chemicals in tissues can be bound to the tissues and unbound. Plasma protein and tissue bindings have significant impact on the toxicokinetics of chemicals. We assumed that only the free, unbound fraction of PGME in blood was available for metabolism and for passive diffusion through the BBB. We also assumed that the unbound fraction in brain might be responsible for any effects in the brain (Mensch et al., 2009). We calculated the unbound PGME concentrations in plasma and in brain tissue using $f_{u,p}$ and $f_{u,b}$ values from our rapid equilibrium dialysis assays. The PGME unbound fraction in blood ($f_{u,blood}$) was calculated by dividing $f_{u,p}$ by the blood-to-plasma ratio (BP). BP was predicted using Uchimura et al. (2010) linear model for neutral chemicals:

$$BP = \frac{C_{blood}}{C_{plasma}} = \left(K_b \times f_p - 1\right) \times \mathrm{Ht} + 1$$

where $f_p$ was the unbound fraction in plasma, Ht was the haematocrit fraction (set at a value of 0.45), and $K_b$ was the red blood cell concentration to the unbound plasma concentration ratio. $K_b$ was predicted using the linear regression formula between log $((1 - f_{u,p})/ f_{u,p})$ and log$K_b$ for neutral compounds, with intercept and slope values of 0.249 and 0.683, respectively.

Model parameter values were from Hopf et al. (2012). All additional physico-chemical and physiological parameters used in our model are listed in Table 2. The urinary excretion-related parameters and metabolism-related parameters were adjusted for aging participants (>58 years), following the approach of Hopf et al. (2012) and Tomicic and Droz (2009). The more time-intensive rich datasets among the *in vivo* datasets available in the literature were used for parameter estimation. Michaelis-Menten maximum rates and constants for phase I metabolism were fitted to blood data from Jones et al. (1997) and Devanthéry et al. (2002). Phase II metabolism parameters ($V_{max2}$, $K_{m2}$) and PGME renal clearance were fitted to Tomicic and Vernez (2014) and Devanthéry et al. (2002) urine data. Key information on the *in vivo* datasets used for model calibration is summarized in Table 3. GetData Graph Digitizer (v. 2.26.0.20) was used to extract pharmacokinetic data from figures in published studies. The model was run in Berkley Madonna software, version 8.3.18, University of California, USA. Parameter fitting was done with Berkeley Madonna curve-fitting tool.

#### 2.4.2. Model evaluation

The model was evaluated using the pharmacokinetic datasets that were not applied in the model calibration. Key information on each of the pharmacokinetic datasets used for model evaluation is summarized in Table 3. Model performance was assessed using the WHO criteria that considers a model acceptable if its predicted values generally match with the experimental kinetic profiles within a two-fold difference (WHO and IPCS, 2010). Goodness-of-fit between observed and simulated concentration values was assessed by linear

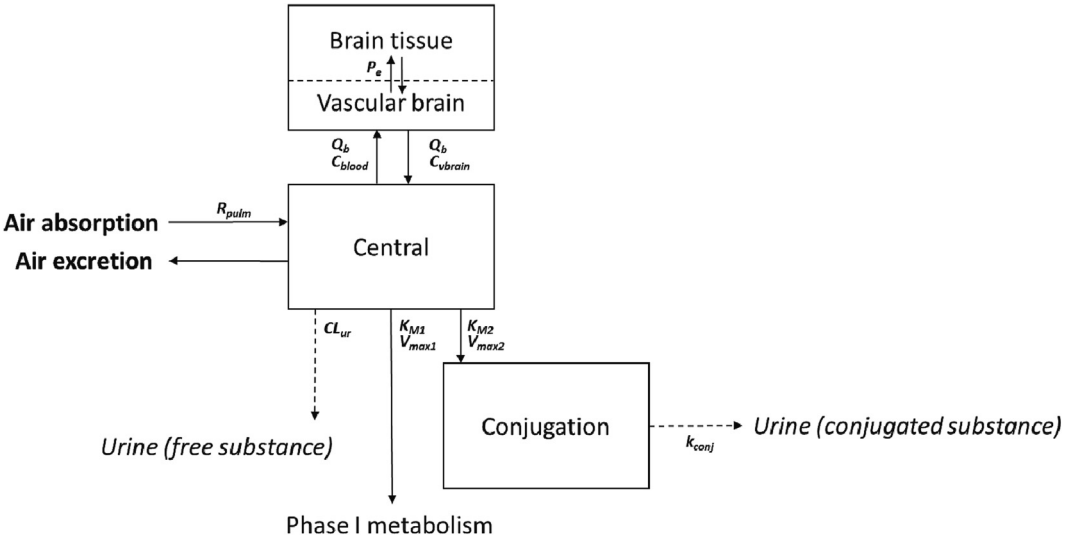


**Fig. 2.** PGME TK model developed in the present study, based on the model of Hopf et al. (2012). Arrows represent flow rates, expressed as mg/h, and rectangles represent model compartments.
Abbreviations for model parameters: $R_{pulm}$ = pulmonary retention, $Q_b$ = cardiac output to brain, $C_{blood}$ = PGME concentration in blood, $C_{vbrain}$ = PGME concentration in brain vascular space, $P_e$ = BBB permeability coefficient, $CL_{ur}$ = urinary clearance, $V_{max1}$ and $K_{M1}$ = maximum velocity and Michaelis-Menten constant for phase I metabolism, $V_{max2}$ and $K_{M2}$ = maximum velocity and Michaelis-Menten constant for phase II metabolism, $K_{conj}$ = urinary excretion rate constant for conjugated PGME.

**Table 2**
Parameters used in the PGME toxicokinetic model that were in addition to the ones already reported in Hopf et al. (2012). The values for metabolic parameters $V_{max1}$, $K_{M1}$, $V_{max2}$, $K_{M2}$, and for $P_{ca}$ replace the ones reported by Hopf et al. (2012).

| Parameters | Symbol | Units | Value | References |
|---|---|---|---|---|
| Physiological parameters | | | | |
| Volume of vascular brain, as fraction of brain volume | FVvb | – | 0.07 | ICRP (1974) |
| Volume of extravascular brain, as fraction of brain volume | FVevb | – | 1-FVvb | ICRP (1974) |
| Volume fraction of brain tissue (as percent of body weight) | FVB | – | 0.02 | Brown et al. (1997) |
| BBB surface | Sh | $cm^2$ | $2 \times 10^5$ | Wong et al. (2013) |
| Fraction of cardiac output in brain at rest / at light work | $BF_{brainrest}/BF_{brain}$ | – | 0.0731/0.12 | Jongeneelen and ten Berge (2011) |
| Chemical-specific parameters | | | | |
| Pulmonary retention | $R_{pulm}$ | – | 0.813 | Kumagai et al. (1999) |
| Octanol-water partition coefficient | $logK_{ow}$ | – | −0.49 | Predicted[b] |
| Central compartment – air partition coefficient | $P_{ca}$ | – | 4555 | Corley et al. (2005) |
| Blood – air partition coefficient | $P_{ba}$ | – | 7107 | Corley et al. (2005) |
| Brain – blood partition coefficient | PBR | – | 0.8 | Predicted[c] |
| Blood-to-plasma ratio | BP | – | 0.94 | Predicted[d] |
| Michaelis-Menten max rate for PGME phase I metabolism | $V_{max1}$ | $mg/(h*kg^{0.75})$ | 17 | Fitted[a] |
| Michaelis-Menten constant for PGME phase I metabolism | $K_{M1}$ | mg/L | 27 | Fitted[a] |
| Michaelis-Menten max rate for PGME conjugation | $V_{max2}$ | $mg/(h*kg^{0.75})$ | 0.12 | Fitted[a] |
| Michaelis-Menten constant for PGME conjugation | $K_{M2}$ | mg/L | 136 | Fitted[a] |
| Renal clearance | $CL_{ur}$ | $l/h/kg^{-0.3}$ | 0.26 | Fitted[a] |
| Unbound fraction in plasma | $f_{u,p}$ | – | 0.54 | Measured |
| Unbound fraction in rat brain homogenate | $f_{u,b}$ | – | 0.36 | Measured |
| Permeability coefficient (BBB) | $P_e$ | cm/min | $10.96 \times 10^{-3}$ | Measured |

[a] Fitted by calibration to *in vivo* human studies Jones et al. (1997), Tomicic and Vernez (2014), Devanthéry et al. (2002).
[b] Data generated by EPA EpiSuite™ through www.chemspider.com.
[c] Value predicted following the approach by DeJongh et al. (1997).
[d] Value predicted following Uchimura et al. (2010) linear regression.

regression, and was considered acceptable when the coefficient of determination ($R^2$) was equal or higher than 0.75 (Yuan et al., 2022). Goodness-of-fit was also assessed by mean absolute percentage error (MAPE) based on these criteria: acceptable if MAPE <50 %, good if MAPE <20 % and > 10 %, excellent if MAPE <10 % (Lin et al., 2017). Linear regression and MAPE were calculated with Microsoft Excel 2016.

### 2.4.3. Sensitivity analysis and uncertainty analysis

A sensitivity analysis was performed to identify model parameters (p) that had the greatest influence on the most critical model output, *i.e.* the 24-h area under the curves (AUC) of PGME in urine, blood, and extravascular brain tissue. The sensitivity analysis was performed using MS Excel 2016. In total 23 parameters were subject to sensitivity analysis. Normalized sensitivity coefficients (NSC) of model output to any selected parameter p of the model were calculated as follows:

$$NSC = (\Delta output/output)/(\Delta p/p)$$

where Δoutput and Δp are the differences between output and *p* values, respectively, before and after increasing p by 1 %. Parameters were categorized depending on the influence they had on the output parameters following these criteria: low impact if $|NSC| < 0.2$, medium impact if $0.2 \leq |NSC| < 0.5$, high impact if $|NSC| \geq 0.5$ (WHO and IPCS, 2010).

The uncertainty of parameters with high impact on model output ($|NSC| \geq 0.5$) was qualitatively assessed depending on the parameter source following these criteria (Lin et al., 2015; Teeguarden et al., 2005): low uncertainty, if a parameter value was obtained from human data parameters or verified through successful use in PBPK models; medium uncertainty, if a parameter value was obtained from a different species with a high probability that scaling holds across species; high uncertainty, if a value was not available for a parameter and appropriate assumptions had to be made.

### 2.4.4. Model simulations and in vitro-to-in vivo extrapolations

The model was used to predict unbound PGME brain concentration upon a typical occupational exposure of 8 h per day, 5 days per week, during one week at a 50 W workload at the Swiss occupational exposure limit (OEL) of 100 ppm (forward dosimetry). The model was also used to estimate the PGME air concentration consistent with the NOAEC of the most

**Table 3**
Pharmacokinetic studies on PGME in humans used for model development and evaluation.

| Exposure concentration | Duration | Measured concentration | Matrix | Number of time points | Sampling time range | Reference |
|---|---|---|---|---|---|---|
| Calibration | | | | | | |
| 100 ppm | 8 h with 30′ break after 4 h | $C_{blood\_u}$ | B | 15 | 0–10 h | Jones et al. (1997) |
| | | $C_{urc}$ | U | 8 | 0–24 h | |
| 53.2 ppm | 6 h | $C_{urc}$, $C_{urtot}$ | U | 11 | 0–24 h | Tomicic and Vernez (2014) |
| 50 ppm | 6 h with 30′ break after 3 h | $C_{blood}$ | B | 3 | 0–6 h | Devanthéry et al. (2002) |
| | | $C_{urc}$, $C_{urtot}$ | U | 9 | 0–24 h | |
| Evaluation | | | | | | |
| 100 ppm | 4 h | $C_{urc}$ | U | 5 | 2–11 h | Brooke et al. (1998) |
| | | $C_{blood\_u}$ | B | 1 | 4 h | |
| 15 ppm, 95 ppm | 6 h with 30′ break after 3 h | $C_{urc}$, $C_{urtot}$ | U | 9 | 0–24 h | Devanthéry et al. (2002) |
| | | $C_{blood}$ | B | 3 | 0–6 h | |
| 49.6 ppm | 6 h | $C_{urc}$, $C_{urtot}$ | U | 11 | 0–24 h | Hopf et al. (2012) |
| 39 ppm | 6 h | $C_{blood\_u}$ | B | 14 | 0–7 h | Borgatta et al. (2022) |

Notes: Abbreviations for matrices: B = blood, U = urine; Abbreviations for chemical: $C_{blood\_u}$ = blood concentration of unbound PGME, $C_{blood}$ = blood concentration of bound + unbound PGME, $C_{urc}$ = free PGME in urine, $C_{urtot}$ = conjugated + free PGME in urine.

sensitive marker in our *in vitro* AGGR tests (reverse dosimetry). For reverse dosimetry, we assumed that only the free fraction of PGME in the brain would lead to a toxic effect. Therefore, we assumed that the PGME *in vitro* nominal concentrations to which the brain cells were exposed were equal to the concentrations of unbound (free) PGME in the extravascular brain.

## 3. Results

### 3.1. In vitro neurotoxicity

Quantification of total mRNA content served as a measurement for estimating general cell death, where a decrease in total content would indicate cell death (Thomas et al., 2015). PGBE and PGME treatment resulted in a concentration-dependent decrease, but did not reach statistical significance. EGME treatment showed no changes in mRNA total content (Fig. 3, panel A). The house keeping gene actin (Act) also showed a tendency for concentration-dependent decreased expression in both PGBE and PGME treated samples at concentrations above 1000 ppm. Again, EGME treatment had no effect (Fig. 3, panel A). This indicated that PGME induced minor cytotoxic effects at concentrations above 1000 ppm. EGME-treatment had no significant effect on neuronal marker neurofilament heavy chain (*Nfh*), astrocyte marker glial fibrillary acidic protein (*Gfap*), oligodendrocyte marker myelin basic protein (*Mbp*) or on the cell stress marker heat-shock protein 32 (*Hsp32*). PGBE and PGME both induced a concentration-dependent decrease in *Nfh*, where the strongest effect was observed with PGBE-treatment (Fig. 3, panel B). This indicated that PGBE and PGME induced axonal perturbations. Decreased *Nfh* expression was accompanied by a concentration-dependent increase of *Gfap* for PGBE-treated samples only (Fig. 3, panel B) indicating that only PGBE induced an astroglial reaction. Neither EGME nor PGME affected the expression of *Mbp* or *Hsp32*. PGBE-treatment, however, elicited a decrease in *Mbp* expression at the highest tested concentration indicating that PGBE affected the myelinating oligodendrocytes. This was accompanied by increased cell stress response, as shown by up-regulated *Hsp32* expression (Fig. 3, panel B). All three glycol ethers elicited – to different degrees – a concentration dependent increase in pro-inflammatory cytokine expression, as indicated by increased relative mRNA levels of interleukins 1-beta (*Il-1β*) and 6 (*Il-6*), as well as of tumor necrosis factor alpha (*Tnfα*) suggesting a pro-inflammatory response (Fig. 3, panel C). The type II interferon cytokine interferon-gamma (Infγ) decreased in a concentration-dependent manner, most markedly after treatment with PGBE, but also after EGME- and PGME treatments (Fig. 3, panel C).

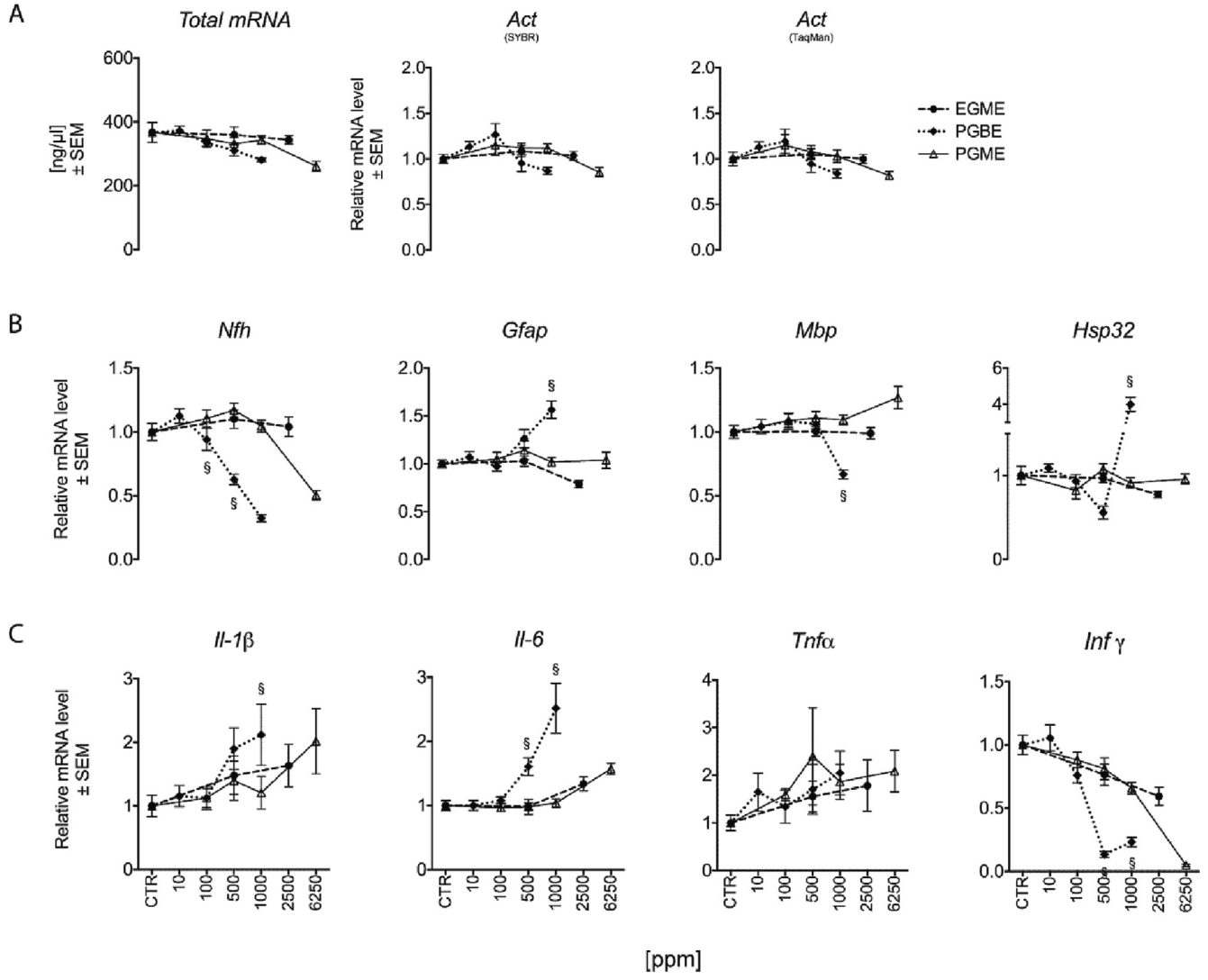


**Fig. 3.** Panel A – total mRNA content in ng/µL (right), and arbitrary units of control for mRNA expression of Actin (Act) as analysed by SYBR Green- or TaqMan technology. Panel B – mRNA expression displayed as arbitrary units of control of neuronal marker Nfh, astroglial marker Gfap, oligodendroglial marker Mbp, and cell stress marker Hsp32. Panel C – mRNA expression displayed as arbitrary units of control of cytokines Il-1β, Il-6, Tnfα, and Infγ. Statistical significance was tested between treatment groups for the same concentrations, and § indicates a *P*-value below 0.05.

**Table 4**
Unbound (free) fraction of EGME, PGBE, and PGME in plasma ($f_{u,p}$) and in rat brain homogenate ($f_{u,b}$).

| Chemical | $f_{u,p}$ | | $f_{u,b}$ | |
|---|---|---|---|---|
| | Mean | SD | Mean | SD |
| EGME | 0.68 | 0.02 | 0.40 | 0.09 |
| PGBE | 0.86 | 0.05 | 0.45 | 0.03 |
| PGME | 0.54 | 0.01 | 0.36 | 0.04 |

### 3.2. CNS distribution

In the dialysis experiments, equilibrium was reached after 5 h, as no difference was observed compared with 7-hour dialysis results (data not shown). Therefore, $f_{u,b}$ and $f_{u,p}$ were calculated based on compound concentration in donor and receiver chambers after 5 h of dialysis (Table 4).

We explored the ability of the test chemicals to cross the blood-brain barrier (BBB). The high recoveries of the glycol ethers in our BBB transport assays indicated the absence of excessive non-specific binding to cell culture materials or metabolism in the cells in these experiments. In the *in vitro* human BBB model (Cecchelli et al., 2014b), EGME, PGBE and PGME showed high BBB permeability when compared to the mean $P_e$ values for NaFlu ($0.7 \times 10^{-3}$ cm/min). NaFlu was used to evaluate the tightness of the *in vitro* BBB (Table 5). In addition, the possible interactions of PGME, PGBE and EGME with efflux transporters expressed at the BBB was tested by their ability to affect the excretion rate of rhodamine 123 (R123) out of Caco-2 cells using the methodology described by Sevin et al. (2019) (supplementary information). None of the glycol ethers tested at 50 μM had any effect on the excretion rate of rhodamine 123 (R123) out of Caco-2 cells (Supplementary fig. S1). In comparison, the well known ABCB1 and ABCG2 inhibitor verapamil at the same concentration reduced the excretion rate of R123 by 75 %. These results indicated the absence of interaction of the tested glycol ethers with ABC transporters such as ABCG2 and ABCC1 which participate in the active efflux of R123 out of the cells.

### 3.3. PGME toxicokinetic model

#### 3.3.1. Model calibration

The TK model was used to simulate PGME concentrations in blood and urine under different exposure durations and concentrations according to different datasets listed in Table 3. $V_{max1}$, $K_{M1}$, $CL_{ur}$, $V_{max2}$, and $K_{M2}$ values were fitted to the datasets selected for calibration. The values of fitted parameters are listed in Table 2. Model predictions for the different datasets are shown in Fig. 4. Overall, the model adequately simulated human pharmacokinetic data of different studies with different exposure doses, exposure duration, and age of the participants, with a coefficient of determination ($R^2$) of 0.92 and a MAPE of 29 %.

#### 3.3.2. Model evaluation

The human TK data not used for model calibration were used for model evaluation. Measured concentrations of PGME in blood and urine were compared with values predicted by the model (Fig. 5). Model predictions correlated well with observed data in urine and blood with $R^2 = 0.96$ and a MAPE of 42 %. 87 % of predictions were within 2-fold error from observed data. Goodness-of-fit increased to $R^2 = 0.99$ and a MAPE of 7 % for predicted *vs.* observed data in blood only.

**Table 5**
Mean (±SD) human brain endothelial-cell permeability coefficient ($P_e \times 10^{-3}$, cm/min) determined *in vitro* for sodium fluorescein (NaFlu) and for the tested glycol ethers (GE) EGME, PGBE, and PGME. NaFlu's $P_e$ was determined in absence (control) as well as in presence of EGME, PGBE, and PGME.

| Condition | $P_e$ NaFlu ($\times 10^{-3}$) | | $P_e$ GE ($\times 10^{-3}$) | |
|---|---|---|---|---|
| | Mean | SD | Mean | SD |
| Control | 0.76 | 0.07 | | |
| EGME | 0.65 | 0.02 | 6.04 | 1.31 |
| PGBE | 0.70 | 0.05 | 8.97 | 2.83 |
| PGME | 0.70 | 0.04 | 10.96 | 2.08 |

#### 3.3.3. Model simulations and in vitro-to-in vivo extrapolations

Modelled brain and blood concentrations of unbound PGME upon a temporal occupational exposure at the OEL and 50 W workload are illustrated in Fig. 6. The maximal unbound and total PGME concentrations in the extravascular brain were 0.33 mM (32 ppm) and 0.92 mM (90 ppm), respectively, at the end of the exposure. The concentration of PGME vapors in air necessary to reach a free PGME concentration in the extravascular brain equal to the NOAEC for *Nfh* (1000 ppm = 10.2 mM) was 684 ppm.

#### 3.3.4. Sensitivity and uncertainty analyses

Fig. 7 shows the results of the sensitivity analysis, namely the parameters with medium or high impact ($|NSC| \geq 0.2$) on the selected output. Selected output was the AUC of unbound PGME in blood and in extravascular brain ($AUC_{blood\_u}$, $AUC_{evb\_u}$), as well as the AUC of free and total PGME in urine ($AUC_{urc}$, and $AUC_{urctot}$). All four selected AUC outputs were highly sensitive to cardiac output ($QCC_{rest}$), Michaelis-Menten kinetic parameters for phase I metabolism ($V_{max1}$, $K_{M1}$), and PGME pulmonary retention ($R_{pulm}$). Additionally, $AUC_{evb\_u}$ was highly sensitive to extravascular brain/blood partition coefficient (PBR), and to blood-to-plasma ratio (BP). AUC of free PGME ($AUC_{urc}$) and total PGME ($AUC_{urtot}$) concentrations in urine were both highly sensitive to renal clearance ($CL_{ur}$) and urinary excretion rate constant ($K_{ur}$). $AUC_{urtot}$ was also highly sensitive to phase II metabolism parameters ($V_{max2}$, $K_{M2}$).

Among the parameters with high impact, those with medium uncertainty were $V_{max1}$, $K_{M1}$. The values for these parameters had been determined in rats, and scaled to humans by Corley et al. (2005). Blood-to-plasma ratio (BP) was estimated to have high uncertainty because it was calculated using a predictive approach that had been verified for drug data in humans. All the other parameters with high impact ($QCC_{rest}$, BW, $K_{ur}$, $R_{pulm}$, $CL_{ur}$) had low uncertainty.

## 4. Discussion

In this study we have assessed the adverse effects of three glycol ethers on rat brain cell markers and have observed that PGBE had the highest potential for neurotoxicity in humans. Also, using a simple TK model we were able to predict PGME brain concentrations in workers upon simulated occupational inhalation exposure to PGME vapors. The calculated PGME brain concentrations at 100 ppm, 8 h per day over five days were 31 times below the NOAEC for neurotoxicity in the AGGR cultures. We also predicted that the PGME air concentrations leading to PGME's brain NOAEC were 7 times above the current occupational exposure limit for PGME.

### 4.1. Neurotoxicity

Upon repeated administration for five days, PGBE was the most potent among the three tested glycol ethers, producing adverse effects on neurons at 100 ppm (0.7 mM), and on astrocytes and oligodendrocytes at 1000 ppm (6.7 mM) (Fig. 3B). PGME produced adverse effects on neurons at 6250 ppm (63.7 mM), which could be explained by its minor cytotoxic effects at concentrations above 1000 ppm (Fig. 3A). EGME did not produce any significant change in the expression of the tested biomarkers. NOAECs for the neurotoxicity endpoint were derived from the dose-response curves (Fig. 3B): 10 ppm (0.07 mM) for PGBE, 1000 ppm (10.2 mM) for PGME and 2500 ppm (31.7 mM) for EGME. It is important to stress that these are brain concentrations.

These results are important because they show the potential neurotoxicity of PGBE - a glycol ether that is widely used in industrial and commercial products. Published data on PGBE neurotoxicity are very limited. Two studies by one research team showed lethargy, CNS depression and hypopnoea in rats after acute oral administration of PGBE (doses not available)

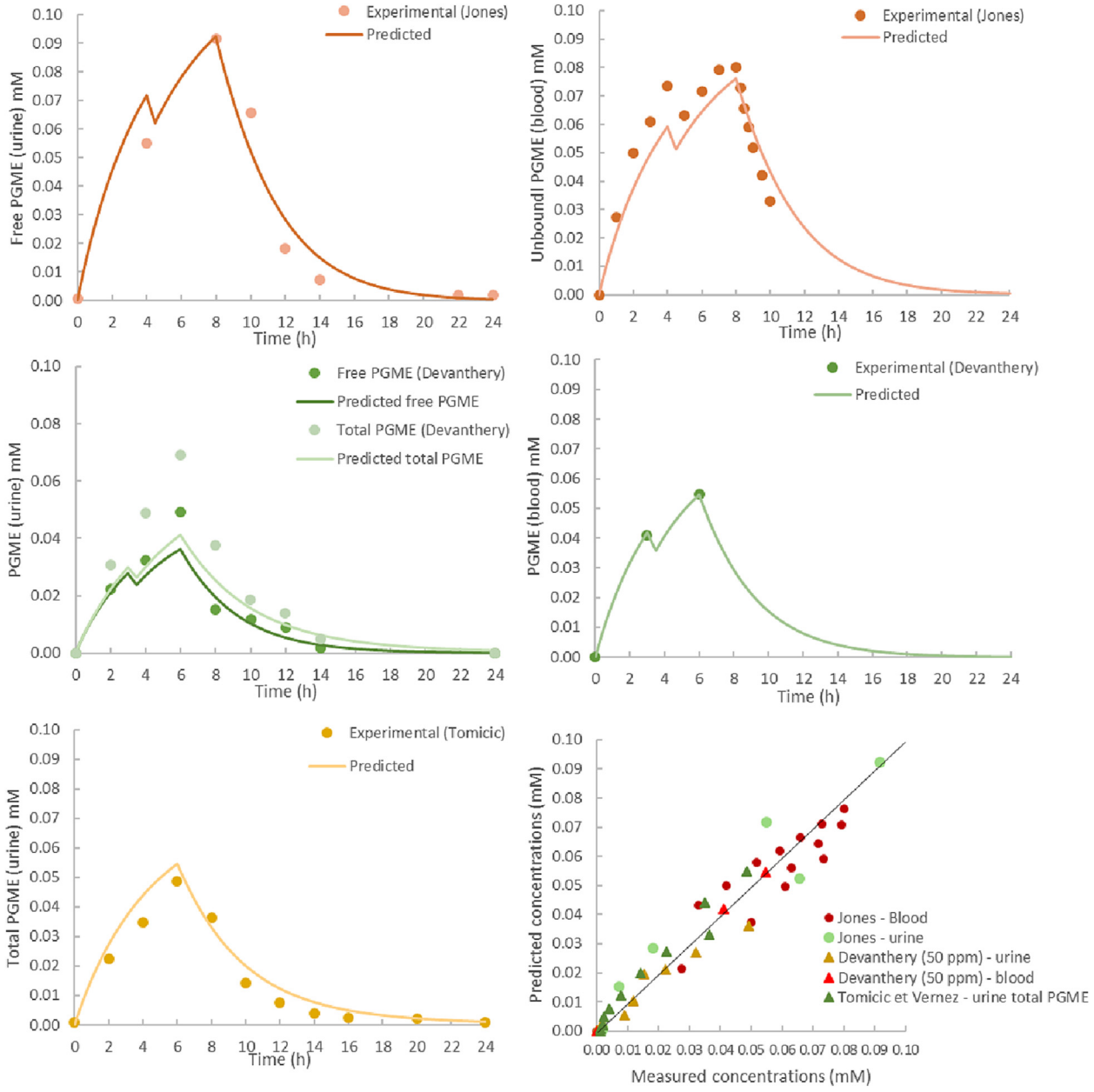


**Fig. 4.** Model calibration: comparison of predicted (lines) *versus* experimental data (dots) for different studies. Plot of measured PGME concentrations in blood and urine *versus* concentrations predicted by our TK model for all studies used for model calibration. The dip in concentration at 3 or 4 h observed in some of the graphs is due to a 30-min break from exposure as described in Table 3.

(Reijnders et al. (1987) as reported by ECETOC (2005a, 2005b)), and no effects in rats after PGBE skin and inhalation exposure (doses not available) (Reijnders and Verschuuren (1987), as reported by ECETOC (2005b)). Considering the limited knowledge on PGBE effects on the brain, and the fact that no OEL has been established for this substance, we suggest that the potential PGBE neurotoxicity be further studied. Moreover, it is interesting to observe that EGME - a glycol ether that has been well recognized for effects in the CNS and PNS in humans (ECETOC, 2005a, 2005b) - has no effects in our brain model. It has been hypothesized that EGME neurological effects could be mediated by its main metabolite, methoxyacetic acid (MAA) (Zavon (1963), as reported by ECETOC (2005a, 2005b)). MAA is produced during EGME metabolism by ADH and ALDH enzymes. The 3D rat brain cell cultures used in our study have some metabolic potential, as they contain different isoforms of cytochrome P450 enzymes (Vichi et al., 2015) but neither ADH nor ALDH. Therefore, it is likely that MAA was not present in our 3D rat brain cell cultures. This could support Zavon (1963)'s hypothesis.

It must be highlighted that all three glycol ethers produced a concentration-dependent increase in pro-inflammatory cytokine expressions Il-1β, Il-6, and TNf-α, and a concentration-dependent decrease in Infγ expression (Fig. 3C). In the healthy brain, immune responses are kept to a minimum. In contrast, different types of CNS injury, including neurotoxic insults, can activate astrocytes and microglial cells, which alter the expression of bioactive factors, among which there are some pro-inflammatory and anti-inflammatory cytokines (Monnet-Tschudi et al., 2007). Pro-inflammatory cytokines induce the expression of major histocompatibility complex (MHC) molecules in brain cells, which gain antigen-presenting capacity. Consequently, brain cells are recognized as a target by invading antigen-specific T lymphocytes. Hence, the observed increase in pro-inflammatory cytokine expression was expected upon exposure to neurotoxicants. On the other hand, the observed down-regulation of Infγ could seem contradictory, considering that it is a pro-inflammatory cytokine. One possible explanation is that normal physiologically active neurons suppress Infγ-mediated MHC expression

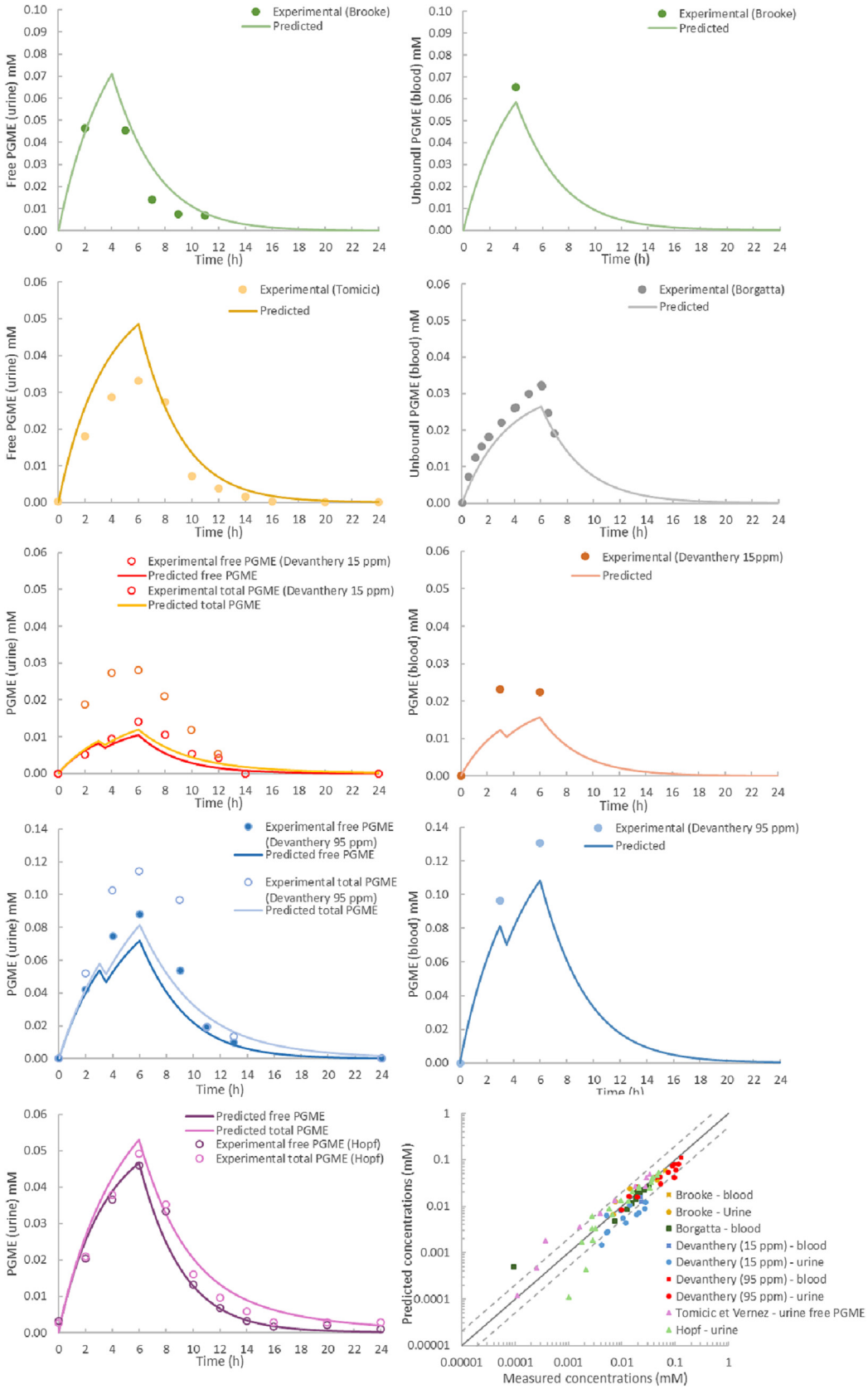


**Fig. 5.** Model evaluation: comparison of predicted (lines) *versus* experimental data (dots) for different studies. Plot of measured PGME concentrations in blood and urine *versus* concentrations predicted by our TK model for all studies used for model evaluation (straight black line is unity, dashed lines represent 2-fold errors). The dip in concentration at 3 or 4 h observed in some of the graphs is due to a 30-min break from exposure as described in Table 3.

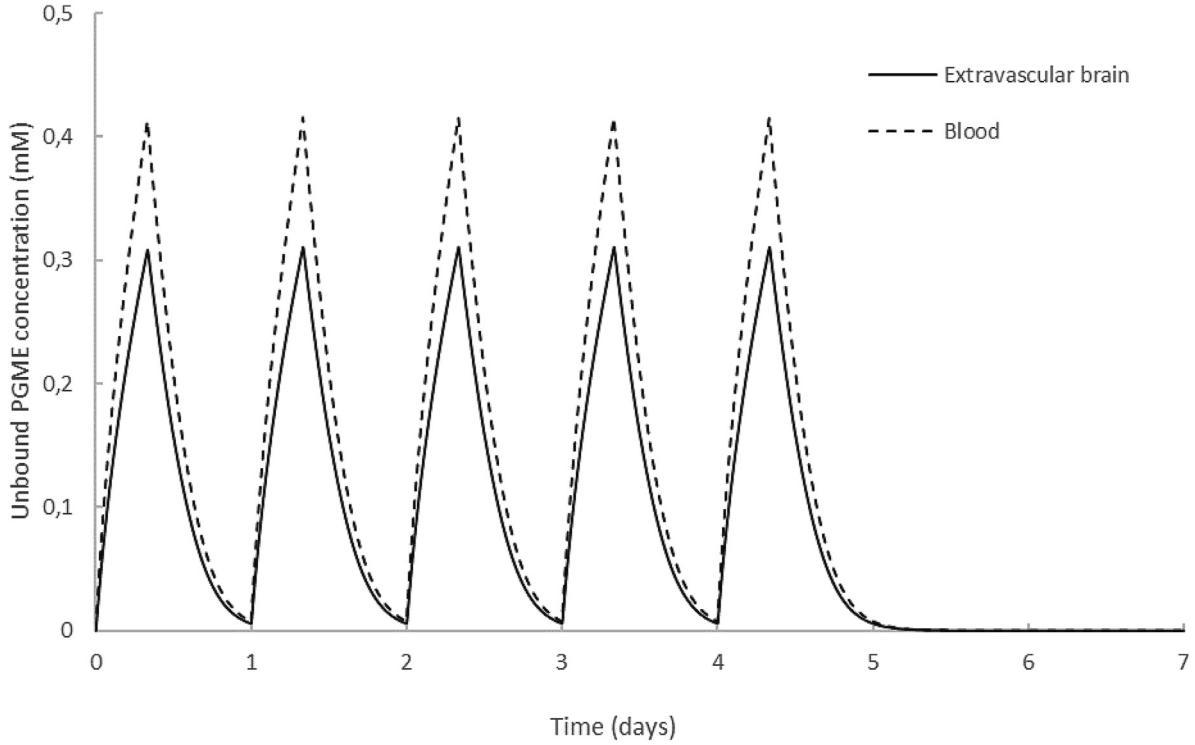


**Fig. 6.** Simulation of brain and blood levels of unbound PGME in workers upon exposure to 100 ppm PGME during 8 h per day, 5 days per week at 50 W workload.

in microglia and astrocytes (Neumann, 2001). This prevents and limits the development of inflammatory responses, as well as of unwanted immune-mediated damage of neurons. So, the opposite tendency that Infγ had compared to Il-1β, Il-6, and TNf-α could be representative of the balance between pro-inflammatory cytokines up-regulation and the counter-regulation of immune response in the CNS (Neumann, 2001). The outcome of the inflammatory reactions in the brain depends on this balance. In neurodegenerative diseases such as Alzheimer's disease and Parkinson's disease, neurodegeneration *via* pro-inflammatory mediators prevails over the protective or reparative effects on neurons due to long-lasting inflammation (Monnet-Tschudi et al., 2007).

### 4.2. CNS distribution

The ability of the three glycol ethers to permeate across the BBB was evaluated using a human *in vitro* BBB model derived from hematopoietic stem cells. The compounds could be ranked according to their $P_e$ values as follows: PGME ($11.0 \times 10^{-3}$ cm/min) > PGBE ($9.0 \times 10^{-3}$ cm/

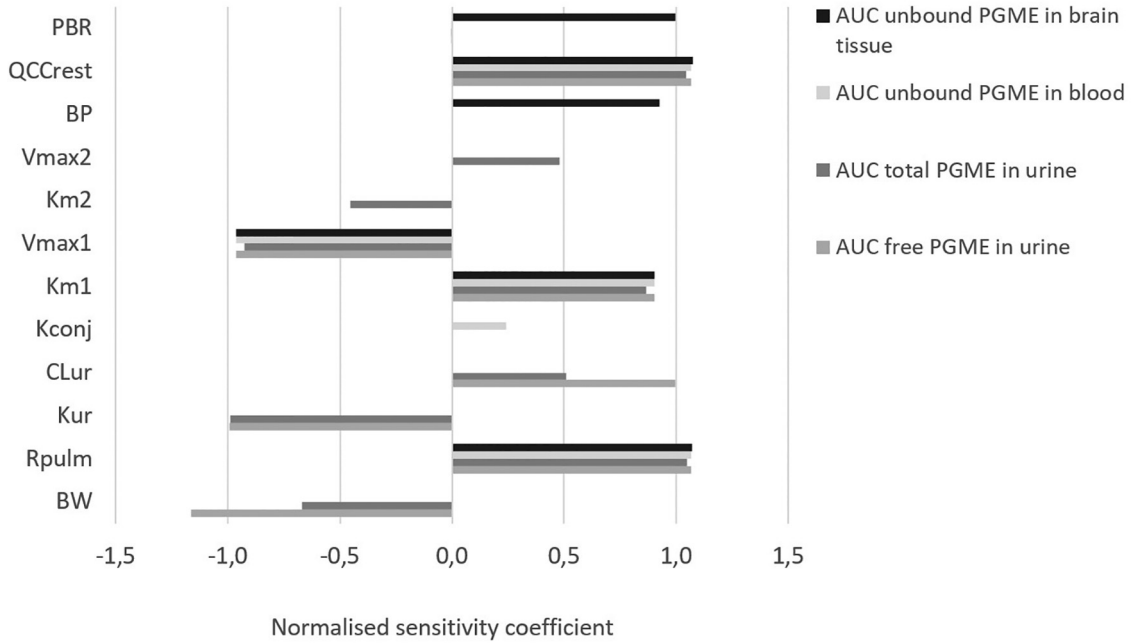


**Fig. 7.** Normalized sensitivity coefficients (NSC) for the area under the concentration curves of unbound PGME in blood (AUCblood_u), unbound PGME in extravascular brain (AUCevb_u), and free (AUCurc) and total (AUCurtot) PGME in urine. Only parameters with medium or high impact on the output ($|NSC| \geq 0.2$) are shown in the graph.

min) > EGME ($6.0 \times 10^{-3}$ cm/min). As a comparison, in the same BBB cell assay the $P_e$ value of the low passive permeable drug atenolol was $1.03 \times 10^{-3}$ cm/min and the one of the highly permeable drug diazepam was $14.57 \times 10^{-3}$ cm/min. The high BBB permeability of the three glycol ethers is in agreement with their expected high passive permeation across cell membrane based on their physico-chemical properties (a molecular weight < 500 Da, <5 hydrogen bond donors, and logP below 5). In addition, no interaction with the ABC efflux pump ABCB1 and ABCG2, known to limit the distribution of compounds across the BBB, could be evidenced. Therefore, given their high BBB permeability, the unbound concentration in brain and plasma of the tested glycol ethers are likely to equilibrate quite fast *in vivo*. Based on their lower $f_{u,b}$ values compared to $f_{u,p}$, the three tested glycol ethers are likely to distribute easily in the brain resulting in higher total concentration in brain than in plasma at equilibration.

### 4.3. TK model

Our TK model could successfully predict PGME blood and urine concentrations from different studies with different participants' age and different exposure concentrations and durations. The model was validated with several different toxicokinetic datasets, showing good results. The uncertainty in brain:blood partition coefficient and in blood-to-plasma ratio suggest that there is some uncertainty in model predictions for brain concentrations. Our TK model predictions of human brain concentrations of unbound PGME upon occupational exposure to PGME vapors at the OEL for one week were 31 times lower than the brain NOAEC for neurotoxicity derived from the AGGR tests (10.2 mM or 1000 ppm). This suggests that occupational exposure to PGME vapors at the OEL for one week may activate the CNS immune response but may not produce any direct adverse effect on brain cells. We directly compared the TK predictions of brain concentrations with the NOAECs obtained in the rat cell-based AGGR assay because this *in vitro* system has been proven to predict acute human brain-specific neurotoxicity. Also, our TK model allowed us to predict the PGME air concentrations ($Cair_{PGME}$ = 684 ppm) necessary to reach the brain NOAEC of 1000 ppm for *Nfh*. These results are in accordance with a human inhalation study of PGME vapor (Stewart et al., 1970), where none of the 23 volunteers exposed to 250 ppm PGME for 7 h had a positive Romberg test or a changed vision. However, Stewart et al. (1970) observed a positive Romberg test at 100 ppm on one out of two volunteers exposed from 1 to 2050 ppm over 2 h. Our results are also in accordance with acute inhalation studies of PGME vapors (Cieszlak and Crissman (1991), as reported by ECETOC (2005a, 2005b)), where concentrations >6000 ppm caused marked sedation in rats and mice, and death in mice. PGME vapors at 3000 ppm caused sedation during the first week of the exposure in subacute studies in rats and mice (Miller et al., 1984; Spencer et al., 2002), in subchronic studies in rats and rabbits (Landry et al. 1983, referenced in ECETOC, 2005a), and in chronic studies in rats and mice (Spencer et al., 2002).

### 4.4. Limitations

Our study has several limitations. First, we used the AGGR to predict brain-specific toxicity upon repeated exposures, even though this *in vitro* system is only validated to detect acute toxicity. Second, we did not take into account metabolism of PGME by CYP450 in AGGR model because AGGR enzymatic activity is deemed to be limited. CYP450 in brain could metabolize PGME to propylene glycol, leading to brain concentrations and effects lower than those predicted by our models. Third, besides the assumptions in the original PGME model which are fully described in Hopf et al. (2012), our TK model did not include the equations to describe metabolism in the brain. Fourth, brain concentrations were not calibrated/validated due to lack of *in vivo* human brain studies on GE's. However, the development of the brain compartment takes into account the diffusion through the BBB, which is based on experimental data. Finally, in the *in vitro-to-in vivo* extrapolations, the nominal PGME concentrations in our *in vitro* assays were considered as equivalent to *in vivo* free concentrations in brain. This assumption was made because our *in vitro* system did not contain any plasma. Therefore, it was assumed that the nominal concentration of the chemical applied *in vitro* was all in its free form. However, the distribution of PGME in our *in vitro* system, especially after repeated exposure, requires further investigation. The distribution study shall include the quantification of the tested chemicals in the cells, cell culture medium, headspace, and on the *in vitro* system's walls. These assumptions, as well as the uncertainties in the model parameters, should be considered for future further developments of this study.

### 4.5. Outlook

The long-term goal of this study is to systematically screen organic solvents for neurotoxicity. This is a first attempt on developing such a strategy. Our simple TK model can be parameterized for other glycol ethers and, with few modifications, for other organic solvents, *e.g.*, by adding a peripheral compartment representing the fat. Our rat brain cell based AGGR *in vitro* model is a screening tool for human acute neurotoxicity. 3D cultures derived from human induced pluripotent stem cells (iPSC) (Zhong et al., 2020) may be used in the future, when such model will be validated. Moreover, no chronic AGGR protocol exists. Chronic solvent encephalopathy reported for many occupations with solvent exposures is thought to take years of exposure to develop. This is a first attempt to develop an AGGR protocol for repeated exposures. After only five days of exposure, AGGR showed an alteration in the expression of a neuronal marker and some pro-inflammatory cytokines, which may be linked to neurodegenerative outcomes. This is promising, and future studies should consider increasing the length of the exposure to replicate chronic exposures.

We used glycol ethers as our test substance because of their wide presence on the market, and their physico-chemical properties. They are not volatile and can be dissolved in cell culture media. Our attempt is a first step to understand if our approach combining *in vitro* and *in silico* methods is valid. However, many solvents have lower water solubility and higher volatility than glycol ethers. The AGGR *in vitro* system has been tested on a training set of molecules, which included mostly drugs, and several organic solvents (Zurich et al., 2013). None of the tested solvents had both characteristics: high volatility (methanol, ethanol, acetonitrile, isopropyl alcohol) and high lipophilicity (hexachlorobenzene, pentachlorophenol). Therefore, future developments of this strategy for different classes of organic solvents will face new challenges, especially testing highly volatile and lipophilic solvents (*e.g.* tetrachloroethylene, toluene). Determining the chemical distribution of the tested solvents in the different parts of the *in vitro* system will be key for the dose-response neurotoxicity assays and the results of the reverse dosimetry.

## 5. Conclusions

In conclusion, we have assessed the adverse effects of three glycol ethers on rat brain cell markers at non cytotoxic levels. PGBE, a glycol ether for which there is no OEL, has the highest potential for neurotoxicity among the three tested glycol ethers. This result is particularly important because there are very limited data on PGBE neurotoxicity, and there is no OEL. EGME seemed not to be neurotoxic at the tested concentrations, in contrast with reported neurological effects on humans upon exposure to EGME. This suggests that its metabolite, MAA, may be responsible for the neurotoxic effects. Our TK model predicted that occupational exposure to PGME vapor concentrations at the OEL is not likely to produce any immediate adverse effect on brain cells. However, brain inflammation was observed after only five days of exposure to each tested glycol ether separately. Hence, a neurodegenerative effect on the long term for any of the tested GE cannot be excluded. Moreover, in occupational settings these solvents are most often used as a mixture, therefore a cumulative effect cannot not be excluded.

Our results should encourage more studies on the neurotoxicity of PGBE, as well as of EGME's main metabolite, MAA. Moreover, glycol ethers are often used as mixtures, and no data exists on mixed exposure and brain

neurotoxicity. Finally, our simple TK model could be parameterized for PGBE and other glycol ethers to predict their concentrations in the brain. Further studies should be done on brain-specific parameters to validate TK model predictions for the brain.

## Funding

The salary of Marjolein Heymans and Sara Wellens was funded by the European Commission within the framework of Marie Sklodowska-Curie Innovative Training Networks: BtRAIN (H2020-MSCA-ITN-2015, no 675619) and in3 (H2020-MSCA-ITN-2016, no 721975).

## CRediT authorship contribution statement

**Elena Reale:** Code, validation, formal analysis, Writing – Original draft; **Jenny Sandström:** Investigation, writing – review & editing; **Maxime Culot**: Methodology, investigation, writing – review & editing; **Julie Hechon**: Investigation, writing – review & editing; **Sara Wellens**: Investigation, writing – review & editing; **Marjolein Heymans**: Investigation, writing – review & editing; **Florianne Tschudi-Monnet**: Resources, supervision, writing – review & editing; **David Vernez**: Conceptualization, methodology; **Nancy B. Hopf**: Conceptualisation, methodology, formal analysis, writing – review & editing.

## Data availability

Data will be made available on request.

## Declaration of competing interest

The authors declare that they have no known competing financial interests or personal relationships that could have appeared to influence the work reported in this paper.

## Appendix A. Supplementary data

Supplementary data to this article can be found online at https://doi.org/10.1016/j.scitotenv.2023.163767.

## References

Blaauboer, B.J., 2001. Toxicodynamic modelling and the interpretation of in vitro toxicity data. Toxicol. Lett. 120, 111–123. https://doi.org/10.1016/S0378-4274(01)00289-2.

Borgatta, M., Hechon, J., Wild, P., Hopf, N.B., 2021. Influence of collection and storage materials on glycol ether concentrations in urine and blood. Sci. Total Environ. 792, 148196. https://doi.org/10.1016/j.scitotenv.2021.148196.

Borgatta, M., Wild, P., Hopf, N.B., 2022. Blood absorption toxicokinetics of glycol ethers after inhalation: a human controlled study. Sci. Total Environ. 816, 151637. https://doi.org/10.1016/j.scitotenv.2021.151637.

Brooke, I., Cocker, J., Delic, J.I., Payne, M., Jones, K., Gregg, N.C., Dyne, D., 1998. Dermal uptake of solvents from the vapour phase; an experimental study in humans. Ann.Occup. Hyg. 42, 531–540. https://doi.org/10.1093/annhyg/42.8.531.

Brown, R.P., Delp, M.D., Lindstedt, S.L., Rhomberg, L.R., Beliles, R.P., 1997. Physiological parameter values for physiologically based pharmacokinetic models. Toxicol. Ind. Health 13, 407–484.

Cecchelli, R., Aday, S., Sevin, E., Almeida, C., Culot, M., Dehouck, L., Coisne, C., Engelhardt, B., Dehouck, M.-P., Ferreira, L., 2014a. A stable and reproducible human blood-brain barrier model derived from hematopoietic stem cells. PLoS ONE 9, 1–11.

Cecchelli, R., Aday, S., Sevin, E., Almeida, C., Culot, M., Dehouck, L., Coisne, C., Engelhardt, B., Dehouck, M.-P., Ferreira, L., 2014b. A stable and reproducible human blood-brain barrier model derived from hematopoietic stem cells. PLoS ONE 9, e99733. https://doi.org/10.1371/journal.pone.0099733.

Chang, X., Tan, Y.-M., Allen, D.G., Bell, S., Brown, P.C., Browning, L., Ceger, P., Gearhart, J., Hakkinen, P.J., Kabadi, S.V., Kleinstreuer, N.C., Lumen, A., Matheson, J., Paini, A., Pangburn, H.A., Petersen, E.J., Reinke, E.N., Ribeiro, A.J.S., Sipes, N., Sweeney, L.M., Wambaugh, J.F., Wange, R., Wetmore, B.A., Mumtaz, M., 2022. IVIVE: facilitating the use of in vitro toxicity data in risk assessment and decision making. Toxics 10, 232. https://doi.org/10.3390/toxics10050232.

Cieszlak, F.S., Crissman, J.W., 1991. Dowanol PM Glycol Ether: An Acute Vapor Inhalation Study in Fischer 344 Rats. Toxicology Research Laboratory, Health and Environmental Sciences Unpublished report, study K-005539-024.

Corley, R.A., Gies, R.A., Wu, H., Weitz, K.K., 2005. Development of a physiologically based pharmacokinetic model for propylene glycol monomethyl ether and its acetate in rats and humans. Toxicology Letters. Proceedings of the Third International Scientific Symposium on the Health Effects of Glycol Ethers - 2002156, pp. 193–213. https://doi.org/10.1016/j.toxlet.2003.12.078.

Cosmetic Ingredient Review Expert Panel, 2008. Final report on the safety assessment of methoxyisopropanol and methoxyisopropyl acetate as used in cosmetics. Int. J. Toxicol. 27, 25–39. https://doi.org/10.1080/10915810802244439.

Crag, S.T., 2012. Ethers of ethylene glycol and derivatives. In: Bingham, E., Cohrssen, B. (Eds.), Patty's Toxicology. John Wiley & Sons Inc, pp. 641–788.

DeJongh, J., Verhaar, H.J., Hermens, J.L., 1997. A quantitative property-property relationship (QPPR) approach to estimate in vitro tissue-blood partition coefficients of organic chemicals in rats and humans. Arch. Toxicol. 72, 17–25.

DeJongh, J., Forsby, A., Houston, J.B., Beckman, M., Combes, R., Blaauboer, B.J., 1999. An integrated approach to the prediction of systemic toxicity using computer-based biokinetic models and biological in vitro test methods: overview of a prevalidation study based on the ECITTS1 project. Toxicol. in Vitro 13, 549–554. https://doi.org/10.1016/S0887-2333(99)00030-2.

Devanthéry, A., Berode, M., Droz, P.-O., 2002. Propylene glycol monomethyl ether occupational exposure. 3. Exposure of human volunteers. Int. Arch. Occup. Environ. Health 75, 203–208. https://doi.org/10.1007/s00420-001-0310-4.

Di, L., Umland, J.P., Chang, G., Huang, Y., Lin, Z., Scott, D.O., Troutman, M.D., Liston, T.E., 2011. Species Independence in brain tissue binding using brain homogenates. Drug Metab. Dispos. 39, 1270–1277. https://doi.org/10.1124/dmd.111.038778.

Dick, F.D., 2006. Solvent neurotoxicity. Occup. Environ. Med. 63, 221–226. https://doi.org/10.1136/oem.2005.022400.

ECETOC, 2005a. Toxicology of Glycol Ethers And Its Relevance to Man (TR095). European Center for Ecotoxicology and Toxicology of Chemicals.

ECETOC, 2005b. Toxicology of Glycol Ethers And Its Relevance to Man (TR 095). European Center for Ecotoxicology and Toxicology of Chemicals.

Evans, E.B., Balster, R.L., 1991. CNS depressant effects of volatile organic solvents. Neurosci. Biobehav. Rev. 15, 233–241. https://doi.org/10.1016/s0149-7634(05)80003-x.

Geldof, M., Freijer, J., van Beijsterveldt, L., Danhof, M., 2008. Pharmacokinetic modeling of non-linear brain distribution of fluvoxamine in the rat. Pharm. Res. 25, 792–804. https://doi.org/10.1007/s11095-007-9390-5.

Honegger, P., Defaux, A., Monnet-Tschudi, F., Zurich, M.G., 2011. Preparation, maintenance, and use of serum-free aggregating brain cell cultures. Methods Mol. Biol. (Clifton N.J.) 758, 81–97. https://doi.org/10.1007/978-1-61779-170-3_6.

Hopf, N.B., Vernez, D., Berthet, A., Charriere, N., Arnoux, C., Tomicic, C., 2012. Effect of age on toxicokinetics among human volunteers exposed to propylene glycol methyl ether (PGME). Toxicol. Lett. 211, 77–84. https://doi.org/10.1016/j.toxlet.2012.02.018.

ICRP, 1974. International Commission on Radiological Protection - Report of the Task Group on the Reference Man.

Jones, K., Dyne, D., Cocker, J., Wilson, H.K., 1997. A biological monitoring study of 1-methoxy-2-propanol: analytical method development and a human volunteer study. Sci. Total Environ. 199, 23–30.

Jongeneelen, F.J., ten Berge, W., 2011. A generic, cross-chemical predictive PBTK model with multiple entry routes running as application in MS Excel; design of the model and comparison of predictions with experimental results. Ann. Occup. Hyg. 55, 841–864. https://doi.org/10.1093/annhyg/mer075.

Kalvass, J.C., Maurer, T.S., Pollack, G.M., 2007. Use of Plasma And Brain Unbound Fractions to Assess the Extent of Brain Distribution of 34 Drugs: Comparison of Unbound Concentration Ratios to In Vivo P-Glycoprotein Efflux Ratios ABSTRACT. 35, pp. 660–666. https://doi.org/10.1124/dmd.106.012294.

Kasteel, E.E.J., Lautz, L.S., Culot, M., Kramer, N.I., Zwartsen, A., 2021. Application of in vitro data in physiologically-based kinetic models for quantitative in vitro-in vivo extrapolation: a case-study for baclofen. Toxicol. in Vitro 76, 105223. https://doi.org/10.1016/j.tiv.2021.105223.

Keski-Säntti, P., Kaukiainen, A., Hyvärinen, H.-K., Sainio, M., 2010. Occupational chronic solvent encephalopathy in Finland 1995–2007: incidence and exposure. Int. Arch. Occup. Environ. Health 83, 703–712. https://doi.org/10.1007/s00420-009-0493-7.

Kinsner-Ovaskainen, A., Prieto, P., Stanzel, S., Kopp-Schneider, A., 2013. Selection of test methods to be included in a testing strategy to predict acute oral toxicity: an approach based on statistical analysis of data collected in phase 1 of the ACuteTox project. Toxicol. in Vitro 27, 1377–1394. https://doi.org/10.1016/j.tiv.2012.11.010.

Kumagai, S., Oda, H., Matsunaga, I., Kosaka, H., Akasaka, S., 1999. Uptake of 10 polar organic solvents during short-term respiration. Toxicol. Sci. 48, 255–263. https://doi.org/10.1093/toxsci/48.2.255.

Lin, Z., Monteiro-Riviere, N.A., Riviere, J.E., 2015. A physiologically based pharmacokinetic model for polyethylene glycol-coated gold nanoparticles of different sizes in adult mice. Nanotoxicology, 1–11 https://doi.org/10.3109/17435390.2015.1027314.

Lin, Z., Jaberi-Douraki, M., He, C., Jin, S., Yang, R.S.H., Fisher, J.W., Riviere, J.E., 2017. Performance assessment and translation of physiologically based pharmacokinetic models from acslX to Berkeley Madonna, MATLAB, and R language: oxytetracycline and gold nanoparticles as case examples. Toxicol. Sci. 158, 23–35. https://doi.org/10.1093/toxsci/kfx070.

Livak, K.J., Schmittgen, T.D., 2001. Analysis of relative gene expression data using real-time quantitative PCR and the 2(-Delta Delta C(T)) Method. Methods 25, 402–408. https://doi.org/10.1006/meth.2001.1262.

Loizou, G., McNally, K., Paini, A., Hogg, A., 2021. Derivation of a human in vivo benchmark dose for bisphenol a from ToxCast in vitro concentration response data using a computational workflow for probabilistic quantitative in vitro to in vivo extrapolation. Front. Pharmacol. 12, 754408. https://doi.org/10.3389/fphar.2021.754408.

Louisse, J., de Jong, E., van de Sandt, J.J.M., Blaauboer, B.J., Woutersen, R.A., Piersma, A.H., Rietjens, I.M.C.M., Verwei, M., 2010. The use of in vitro toxicity data and physiologically based kinetic modeling to predict dose-response curves for in vivo developmental toxicity of glycol ethers in rat and man. Toxicol. Sci. 118, 470–484. https://doi.org/10.1093/toxsci/kfq270.

Mensch, J., Oyarzabal, J., Mackie, C., Augustijns, P., 2009. In vivo, in vitro and in silico methods for small molecule transfer across the BBB. J. Pharm. Sci. 98, 4429–4468. https://doi.org/10.1002/jps.21745.

Mikkelsen, S., Jørgensen, M., Browne, E., Gyldensted, C., 1988. Mixed solvent exposure and organic brain damage. A study of painters. Acta Neurol. Scand. Suppl. 118, 1–143.

Miller, R.R., Hermann, E.A., Young, J.T., Landry, T.D., Calhoun, L.L., 1984. Ethylene glycol monomethyl ether and propylene glycol monomethyl ether: metabolism, disposition, and subchronic inhalation toxicity studies. Environ. Health Perspect. 57, 233–239. https://doi.org/10.1289/ehp.8457233.

Monnet-Tschudi, F., Zurich, M.-G., Honegger, P., 2007. Neurotoxicant-induced inflammatory response in three-dimensional brain cell cultures. Hum. Exp. Toxicol. 26, 339–346. https://doi.org/10.1177/0960327107074589.

Neumann, H., 2001. Control of glial immune function by neurons. Glia 36, 191–199. https://doi.org/10.1002/glia.1108.

Noorlander, A., Zhang, M., van Ravenzwaay, B., Rietjens, I.M.C.M., 2022. Use of physiologically based kinetic modeling-facilitated reverse dosimetry to predict in vivo acute toxicity of tetrodotoxin in rodents. Toxicol. Sci. 187, 127–138. https://doi.org/10.1093/toxsci/kfac022.

Prieto, P., Kinsner-Ovaskainen, A., Stanzel, S., Albella, B., Artursson, P., Campillo, N., Cecchelli, R., Cerrato, L., Díaz, L., Di Consiglio, E., Guerra, A., Gombau, L., Herrera, G., Honegger, P., Landry, C., O'Connor, J.E., Páez, J.A., Quintas, G., Svensson, R., Turco, L., Zurich, M.G., Zurbano, M.J., Kopp-Schneider, A., 2013. The value of selected in vitro and in silico methods to predict acute oral toxicity in a regulatory context: results from the European project ACuteTox. Toxicol. in Vitro 27, 1357–1376. https://doi.org/10.1016/j.tiv.2012.07.013.

Punt, A., Aartse, A., Bovee, T.F.H., Gerssen, A., van Leeuwen, S.P.J., Hoogenboom, R.L.A.P., Peijnenburg, A.A.C.M., 2019. Quantitative in vitro-to-in vivo extrapolation (QIVIVE) of estrogenic and anti-androgenic potencies of BPA and BADGE analogues. Arch. Toxicol. 93, 1941–1953. https://doi.org/10.1007/s00204-019-02479-6.

Reijnders, J., Verschuuren, H., 1987. Evaluation of the Acute Dermal Toxicity of Dowanol PnB in the Rat. RCC Notox, 's-Hertogenbosch, Netherlands Unpublished report 066/873.

Reijnders, J., Zucker-Keiser, A., Verschuuren, H., 1987. Evaluation of the acute oral toxicity of Dowanol PnB in the rat. Toxicol. Res. lab. Report.

Ridgway, P., Nixon, T.E., Leach, J.-P., 2003. Occupational exposure to organic solvents and long-term nervous system damage detectable by brain imaging, neurophysiology or histopathology. Food Chem. Toxicol. 41, 153–187. https://doi.org/10.1016/s0278-6915(02)00214-4.

Ryu, S., Tess, D., Chang, G., Keefer, C., Burchett, W., Steeno, G.S., Novak, J.J., Patel, R., Atkinson, K., Riccardi, K., Di, L., 2020. Evaluation of fraction unbound across 7 tissues of 5 species. J. Pharm. Sci. 109, 1178–1190. https://doi.org/10.1016/j.xphs.2019.10.060.

Sainio, M.A., 2015. Chapter 7 - neurotoxicity of solvents. In: Lotti, M., Bleecker, M.L. (Eds.), Handbook of Clinical Neurology, Occupational Neurology. Elsevier, pp. 93–110 https://doi.org/10.1016/B978-0-444-62627-1.00007-X.

Sevin, E., Dehouck, L., Versele, R., Culot, M., Gosselet, F., 2019. A miniaturized pump out method for characterizing molecule interaction with ABC transporters. Int. J. Mol. Sci. 20, 5529. https://doi.org/10.3390/ijms20225529.

Shi, M., Bouwmeester, H., Rietjens, I.M.C.M., Strikwold, M., 2020. Integrating in vitro data and physiologically based kinetic modeling-facilitated reverse dosimetry to predict human cardiotoxicity of methadone. Arch. Toxicol. 94, 2809–2827. https://doi.org/10.1007/s00204-020-02766-7.

Spencer, P.J., Crissman, J.W., Stott, W.T., Corley, R.A., Cieszlak, F.S., Schumann, A.M., Hardisty, J.F., 2002. Propylene glycol monomethyl ether (PGME): inhalation toxicity and carcinogenicity in Fischer 344 rats and B6C3F1 mice. Toxicol. Pathol. 30, 570–579. https://doi.org/10.1080/01926230290105848.

Stewart, R.D., Baretta, E.D., Dodd, H.C., Torkelson, T.R., 1970. Experimental human exposure to vapor of propylene glycol monomethyl ether. Arch.Environ.Health 20, 218–223. https://doi.org/10.1080/00039896.1970.10665577.

Teeguarden, J.G., Deisinger, P.J., Poet, T.S., English, J.C., Faber, W.D., Barton, H.A., Corley, R.A., Clewell III, H.J., 2005. Derivation of a human equivalent concentration for n-butanol using a physiologically based pharmacokinetic model for n-butyl acetate and metabolites n-butanol and n-butyric acid. Toxicol. Sci. 85, 429–446. https://doi.org/10.1093/toxsci/kfi103.

Thomas, M.P., Liu, X., Whangbo, J., McCrossan, G., Sanborn, K.B., Basar, E., Walch, M., Lieberman, J., 2015. Apoptosis triggers specific, rapid, and global mRNA decay with 3' uridylated intermediates degraded by DIS3L2. Cell Rep. 11, 1079–1089. https://doi.org/10.1016/j.celrep.2015.04.026.

Tomicic, C., Droz, P.-O., 2009. Age differences in biological monitoring of chemical exposure: a tentative description using a toxicokinetic model. Int. Arch. Occup. Environ. Health 82, 669–676. https://doi.org/10.1007/s00420-008-0366-5.

Tomicic, C., Vernez, D., 2014. Sex differences in urinary levels of several biological indicators of exposure: a simulation study using a compartmental-based toxicokinetic model. J. Occup. Environ. Hyg. 11, 377–387. https://doi.org/10.1080/15459624.2013.875180.

Triebig, G., Barocka, A., Erbguth, F., Höll, R., Lang, C., Lehrl, S., Rechlin, T., Weidenhammer, W., Weltle, D., 1992. Neurotoxicity of solvent mixtures in spray painters. II. Neurologic, psychiatric, psychological, and neuroradiologic findings. Int. Arch. Occup. Environ. Health 64, 361–372. https://doi.org/10.1007/BF00379547.

Uchimura, T., Kato, M., Saito, T., Kinoshita, H., 2010. Prediction of human blood-to-plasma drug concentration ratio. Biopharm. Drug Dispos. 31, 286–297. https://doi.org/10.1002/bdd.711.

Verwei, M., van Burgsteden, J.A., Krul, C.A.M., van de Sandt, J.J.M., Freidig, A.P., 2006. Prediction of in vivo embryotoxic effect levels with a combination of in vitro studies and PBPK modelling. Toxicol. Lett. 165, 79–87. https://doi.org/10.1016/j.toxlet.2006.01.017.

Vichi, S., Sandström von Tobel, J., Gemma, S., Stanzel, S., Kopp-Schneider, A., Monnet-Tschudi, F., Testai, E., Zurich, M.G., 2015. Cell type-specific expression and localization of cytochrome P450 isoforms in tridimensional aggregating rat brain cell cultures. Toxicol. in Vitro 30, 176–184. https://doi.org/10.1016/j.tiv.2015.03.005.

Wang, Q., Zhu, L., Chen, M., Ma, X., Wang, X., Xia, J., 2017. Simultaneously determination of bisphenol A and its alternatives in sediment by ultrasound-assisted and solid phase extractions followed by derivatization using GC-MS. Chemosphere 169, 709–715. https://doi.org/10.1016/j.chemosphere.2016.11.095.

WHO, IPCS, 2010. Characterization And Application of Physiologically Based Pharmacokinetic Models in Risk Assessment, Harmonization Project Document. World Health Organization, Geneva.

Wong, A.D., Ye, M., Levy, A.F., Rothstein, J.D., Bergles, D.E., Searson, P.C., 2013. The blood-brain barrier: an engineering perspective. Front Neuroeng 6. https://doi.org/10.3389/fneng.2013.00007.

Yuan, L., Chou, W.-C., Richards, E.D., Tell, L.A., Baynes, R.E., Davis, J.L., Riviere, J.E., Lin, Z., 2022. A web-based interactive physiologically based pharmacokinetic (iPBPK) model for meloxicam in broiler chickens and laying hens. Food Chem. Toxicol. 168, 113332. https://doi.org/10.1016/j.fct.2022.113332.

Zavon, M., 1963. Methyl cellosolve intoxication. Am. Ind. Hyg. Assoc. J. 36–41.

Zhong, X., Harris, G., Smirnova, L., Zufferey, V., Sá, R.C.D.S.E., Baldino Russo, F., Baleeiro Beltrao Braga, P.C., Chesnut, M., Zurich, M.G., Hogberg, H.T., Hartung, T., Pamies, D., 2020. Antidepressant paroxetine exerts developmental neurotoxicity in an iPSC-derived 3D human brain model. Front. Cell. Neurosci. 21, 14–25. https://doi.org/10.3389/fncel.2020.00025.

Zurich, M.-G., Stanzel, S., Kopp-Schneider, A., Prieto, P., Honegger, P., 2013. Evaluation of aggregating brain cell cultures for the detection of acute organ-specific toxicity. Toxicol. in Vitro 27, 1416–1424. https://doi.org/10.1016/j.tiv.2012.06.018.